Subconjunctival Lymphatics Respond to VEGFC and Anti-Metabolites in Rabbit and Mouse Eyes

Jong Yeon Lee,[1] Jingyi Wu,[2–4] Yameng Liu,[3,4] Sindhu Saraswathy,[5] Longfang Zhou,[3,4] Qianwen Bu,[3,4] Ying Su,[3,4] Dongwon Choi,[6] Eunkyung Park,[6] Clemens A. Strohmaier,[7,8] Robert N. Weinreb,[8] Young-Kwon Hong,[6] Xiaojing Pan,[3,4] and Alex S. Huang[8]

[1]Department of Ophthalmology, Gachon University College of Medicine, Gil Medical Center, Incheon, Korea
[2]Weifang Medical University, Weifang, Shandong Province, China
[3]State Key Laboratory Cultivation Base, Shandong Provincial Key Laboratory of Ophthalmology, Shandong Eye Institute, Shandong First Medical University & Shandong Academy of Medical Sciences, Qingdao, Shandong Province, China
[4]Qingdao Eye Hospital of Shandong First Medical University, Qingdao, Shandong Province, China
[5]Doheny Eye Institute and Stein Eye Institute, Department of Ophthalmology, David Geffen School of Medicine, University of California, Los Angeles, California, United States
[6]Department of Surgery, Norris Comprehensive Cancer Center Keck School of Medicine, University of Southern California, Los Angeles, California, United States
[7]Department of Ophthalmology, Johannes Kepler University, Linz, Austria
[8]Hamilton Glaucoma Center, The Viterbi Family Department of Ophthalmology, Shiley Eye Institute, University of California, San Diego, California, United States

Correspondence: Xiaojing Pan, State Key Laboratory Cultivation Base, Shandong Provincial Key Laboratory of Ophthalmology, Shandong Eye Institute, Shandong First Medical University & Shandong Academy of Medical Sciences, Qingdao 266071, Shandong Province, China; panxjcrystal@163.com.

JYL and JW contributed equally to this work.

Received: May 8, 2022
Accepted: September 5, 2022
Published: September 27, 2022

Citation: Lee JY, Wu J, Liu Y, et al. Subconjunctival lymphatics respond to VEGFC and anti-metabolites in rabbit and mouse eyes. *Invest Ophthalmol Vis Sci.* 2022;63(10):16. https://doi.org/10.1167/iovs.63.10.16

Purpose. To characterize and pharmacologically influence subconjunctival lymphatics in rabbit and mouse eyes.

Methods. Rabbits received subconjunctival injections of trypan blue or fixable fluorescent dextrans. Bleb-related outflow pathways were quantified. Immunofluorescence for vessel-specific markers (lymphatics [podoplanin and LYVE-1] and blood vessels [CD31]) were performed in native rabbit conjunctiva and after fixable fluorescent dextran injection. Vascular endothelial cell growth factor-C (VEGFC) was injected subconjunctivally in rabbits. mRNA and protein were assessed for the above markers using RT-PCR and Western blot. Alternatively, mouse studies used Prox1-tdTomato transgenic reporter mice. Subconjunctival injection conditions included: no injection, balanced salt solution (BSS), VEGFC, 5-fluorouracil (5FU) and two concentrations of mitomycin-C (MMC). Two mouse injection protocols (short and long) with different follow-up times and number of injections were performed. Mouse eyes were enucleated, flat mounts created, and subconjunctival branching and length assessed.

Results. Rabbit eyes demonstrated clear bleb-related subconjunctival outflow pathways that were distinct from blood vessels and were without nasal/temporal predilection. Immunofluorescence against vessel-specific markers showed lymphatics and blood vessels in rabbit conjunctiva, and these lymphatics overlapped with bleb-related subconjunctival outflow pathways. Subconjunctival VEGFC increased lymphatic ($P = 0.004$–0.04) but not blood vessel ($P = 0.77$–0.84) mRNA or protein in rabbits. Prox1-tdTomato transgenic reporter mice demonstrated natively fluorescent lymphatics. Subconjunctival VEGFC increased murine lymphatic branching and length ($P \leq 0.001$–0.004) while antimetabolites ($P \leq 0.001$–0.043) did the opposite for the long protocol.

Discussion. Subconjunctival lymphatics are pharmacologically responsive to both VEGFC and antimetabolites in two animal models studied using different methodologies. These results may be important for bleb-forming glaucoma surgeries or ocular drug delivery.

Keywords: subconjunctival lymphatics, blebs, glaucoma surgery, aqueous outflow, drug delivery

The subconjunctival space is normally a potential space in the eye. It can become expanded in circumstances of ocular pathology or during treatment of eye diseases. Chemosis is the expansion of the subconjunctival space from total body fluid overload,[1] third-spacing due to oncotic gradient changes,[1] or ocular surface infection/inflammation.[2] To treat eye diseases, subconjunctival antibiotic and steroid injections are often given at the end of eye surgeries as a drug delivery bleb to prevent infection and inflammation.[3] Alternatively, subconjunctival steroids can be used to treat ocular surface inflammatory disorders.[4] In glaucoma surgery, the subconjunctival space is purposely

opened and connected to the anterior chamber by a direct low-resistance communication, resulting in a surgical bleb.[5,6] In all cases, subconjunctival fluid outflow occurs as chemosis, and drug injections blebs eventually resolve; and for glaucoma, surgical bleb fluid outflow is desirable to lower intraocular pressure.

Lymphatics have many important roles in the body including fluid homeostasis and immune surveillance.[7] In the eye and central nervous system, the presence of central nervous system or intraocular lymphatics has been long debated, although recent evidence now support a lymphatic presence or function in these areas.[8–11] Alternatively, the conjunctiva has long been known to be rich in lymphatics.[12,13] Their presence is so well established that consensus agreement on how to define lymphatics in the eye specifically exclude conjunctiva and the subconjunctival space from stringent consensus criteria.[14] However, the purpose of conjunctival lymphatics, their role in ocular pathology, and how to leverage them for potential clinical applications is still under investigation.

Recent research supports that conjunctival lymphatics are responsible for mediating subconjunctival outflow and draining interstitial fluid from the conjunctival stroma. Human case series with inadvertent (traumatic subconjunctival hemorrhage) or advertent subconjunctival tracer application have shown that subconjunctival blebs give rise to irregular sausage-shaped outflow pathways.[15–17] These pathways are distinct from classic Y-shaped ocular surface episcleral veins or corkscrew conjunctival blood vessels.[17,18] Subsequent study in post-mortem porcine eyes in the laboratory isolated these pathways, and they demonstrated immunopositivity for PROX-1 and podoplanin (lymphatic makers) but not CD31 (a blood vessel endothelial marker).[19] Structural evaluation using optical coherence tomography (OCT) in postmortem porcine eyes showed that these bleb-related outflow pathways contained intraluminal valves, a lymphatic hallmark.[19,20] Similar results were seen in human patients who received subconjunctival anesthetic injection (mixed with a fluorescent tracer) prior to clinically indicated intravitreal drug injection for the treatment of retinal diseases.[17] In these cases, the bleb-related outflow pathways of human patients showed irregular sausage-shaped pathways that also contained OCT-visualized valves.

Thus it is of interest to know whether these lymphatics can be influenced. The rabbit is an ideal research model because subconjunctival lymphatics are well established.[12] Moreover, rabbits are a commonly studied trabeculectomy animal model.[21,22] Disadvantages of rabbit research include high cost, resource, and time requirements. Alternatively, mouse research has the advantage of genetic mouse models and the ability to generate many animals to test a greater number of conditions.[23,24] To promote lymphangiogenesis, vascular endothelial growth factor type-C (VEGFC) activates the VEGF receptor-3 pathway[25] and is a known pro-lymphatic growth factor.[26] To limit lymphatics, it has been hypothesized that antimetabolites and the concentrations used during glaucoma surgeries limit lymphatic growth.[27] Therefore we investigate these two animal models using molecular and structural imaging endpoints, and we hypothesize that subconjunctival lymphatics respond to the above pharmacological agents.

Methods

Rabbit Ocular Surface Lymphangiography

For all rabbit experiments, twenty-seven male New Zealand White rabbits (Xi Lingjiao Co., Jinan, China; aged 12-14 weeks; 3-4 kg average body weight) were raised and treated according to Institutional Animal Care protocol SDSYKYJS.No20180036 and the Statement of the Association for Research in Vision and Ophthalmology (ARVO). During this research, two rabbits were excluded because the conjunctiva was damaged during injection, and a bleb could not be formed. Specific sample sizes are below.

Sixteen rabbits were used for trypan blue ocular surface lymphangiography and quantitation of outflow pathways. Rabbits were anesthetized using intravenous sodium pentobarbital (30 mg/kg), and their eyelids were gently opened using forceps after topical anesthesia using 2% ropivacaine hydrochloride (Alcon, Geneva, Switzerland). At the bulbar conjunctiva near the cornea, ~50 µL of tracer was injected subconjunctival in randomly selected eyes using a no. 31G needle to form a 2 to 3 mm bleb. Tracers included 0.5% trypan blue (960.8 molecular weight; Solarbio T8070; Solarbio Life Science, Beijing, China) or 3 mg/mL fixable FITC-dextrans (150 kD; Sigma FD150S; D7136; Burlington, MA, USA). Each tracer was prepared using sterile-filtered PBS (Solarbio P1022; Solarbio). One to two minutes after each injection, the blebs and outflow pathways were imaged using a ZeissSL130 slit lamp biomicroscope using the SL Imaging Module. The slit lamp arm was set at a 45° angle with magnification × 10. A cobalt blue filter was used for the fluorescent dextran imaging.

Quantitative Measurement of Rabbit Conjunctival Lymphatics

Trypan blue is an anionic azo dye, has traditionally been used during cataract surgery as a capsular stain, and can be used to visualize bleb-related outflow pathways.[12,28] To compare subconjunctival outflow on the nasal versus the temporal sides of the eye, ~50 µL microliters of trypan blue were injected subconjunctival on both sides. Images were recorded using a slit-lamp camera. The number of pathways immediately arising from the bleb were counted in a masked fashion and statistically compared using paired *t*-test (SPSS, v22.0; IBM, Armonk, NY, USA).

Rabbit Immunofluorescence Labeling

Three rabbits were used for immunofluorescence studies that also included fixable FITC-dextran tracer, where methods have been previously described.[19,29–31] Briefly, for eyes that received fixable FITC-dextran tracer, the tissue was marked for orientation. The tracer was fixable due to a lysine moiety and with fixation could be attached to the pathways they filled. The conjunctiva near the injection area (including the bleb and outflow pathways) was carefully excised and placed in 4% paraformaldehyde for 15 minutes at room temperature followed by 4°C overnight to trap the tracer. The tissue was embedded in Tissue-Tek (Sakura Fintech, Tokyo, Japan), frozen under liquid nitrogen, and 7 µm cryosections were cut and collected on Superfrost slides (Fisher Scientific, Waltham, MA, USA). Sections were

Investigative Ophthalmology & Visual Science

blocked with 10% donkey serum albumin and permeabilized with 0.3% Triton X-100. The sections were incubated with the primary antibody overnight at 4°C. Antibodies were against podoplanin (a 38 kDa membrane glycoprotein originally identified on podocytes and expressed on the endothelium of lymphatic capillaries but not quiescent or proliferating blood vascular endothelium),[32,33] LYVE-1 (a relatively lymphatic-specific receptor that is expressed on lymphatic but not blood vascular endothelium),[34,35] and CD-31 (a well-established blood vessel endothelial marker). The sections were then incubated with fluorophore-coupled anti-mouse or anti-rabbit secondary antibodies for one hour at room temperature. Secondary antibody labeling alone did not show signal (Supplementary Fig. S1). The 4′6-diamidino-2-phenylindole labeling was performed, and the sections were viewed under a fluorescence microscope (Nikon E800; Nikon Inc., Melville, NY, USA). Primary and secondary antibodies are listed (Supplementary Table S1A).

Rabbit VEGF-C Lymphatic Study

Six normal and healthy New Zealand white rabbits received 20 µL of subconjunctival human recombinant VEGFC (n = 3) (0.05 mg/mL; BioVision 4633; BioVision Inc., Milpitas, CA, USA) diluted in PBS or PBS-alone (n = 3) as a control. Aseptic technique was used with application of topical antibiotic (levofloxacin hydrochloride eye drops [Alcon]) after each injection. Ten days later, rabbits were sacrificed by air embolism after intravenous overdose using sodium pentobarbital. The conjunctiva near the injection was carefully excised and frozen in liquid nitrogen.

Rabbit Western Blot Analyses

Tissue lysates from the above experimental and control conjunctival tissues were made using RIPA lysis buffer containing PMSF (Solarbio; Beijing, China). Samples were cut into small pieces and homogenized (TissueLyser II; Qiagen, Hilden, Germany). This was followed by ultrasonic homogenization (Sonics-VCX 130; Sonics, Newtown, CT, USA). Protein concentration was measured using a BCA protein determination kit (Beyotime P1002; Beyotime Institute of Biotechnology, Jiangsu, China). Lysates were combined with 5 × SDS-PAGE loading buffer (Cowin Bio CW0027; CoWin Bioscience Co., Ltd, Boston, MA, USA), boiled at 95°C for 10 minutes and spun in a centrifuge. Extracts (25 mg or 45 mg) were separated by SDS-PAGE. A 10% concentration gel was prepared using a PAGE gel fast preparation kit (Epizyme PG112; Epizyme Inc., Boston, MA, USA). Gels were run at 80 V for 30 minutes and then at 120V for 60 minutes. This was followed by transfer to polyvinylidene difluoride membranes (Merck Millipore, Burlington, MA, USA). Membranes were blocked for one hour at room temperature using 5% bovine serum albumin and then incubated with primary antibodies overnight at 4°C. Blots were then washed four times in TBS/Tween-20 and incubated with horseradish peroxidase coupled to goat anti-mouse or mouse anti-rabbit secondary antibody for two hours. Anti-rabbit secondary-only conditions were performed. After additional washing, the bands were visualized using an enzyme ECL-chemiluminescence kit (Chemicon, Temecula, CA, USA). Blots were recorded and band image intensity was calculated using ImageJ (http://imagej.nih.gov/ij/; National Institutes of Health, Bethesda, MD, USA). Quantitation was determined relative to GAPDH, and all experiments were conducted at least three separate times. Individual results are shown as mean ± standard error of the mean (SEM) (Supplementary Table S2A). *T*-tests (two-tailed and unpaired) were performed using SPSS v22.0. A value of $P < 0.05$ was considered statistically significant ($^{*}P < 0.05$ and $^{**}P < 0.01$). Primary and secondary antibodies are listed (Supplementary Table S1B).

Rabbit Real-Time qPCR Analysis

Total RNA was also extracted from frozen conjunctival tissues using a Nucleospin RNA Kit (BD Biosciences, Palo Alto, CA, USA). Isolated RNA was reverse transcribed into cDNA using the Primescript First-Strand cDNA Synthesis kit (Vazyme Biotech Co., Ltd, Nanjing, China). Quantitative PCR was performed using SYBR Green reagents (Vazyme Biotech Co., Ltd). The results were analyzed with the Sequence Detection System software (Applied Biosystems, Foster City, CA, USA). For relative quantization, $2^{-\Delta\Delta Ct}$ was calculated and used as a relative index of expression level. RT-qPCR was conducted using the primers according to the manufacturer's protocol (Supplementary Table S1C). GAPDH was used as an internal control. All experiments were conducted at least three separate times. Individual results are shown as mean ± SEM (Supplementary Table S2B). *T*-tests (two-tailed and unpaired) were performed using SPSS v22.0. A value of $P < 0.05$ was considered statistically significant ($^{*}P < 0.05$ and $^{**}P < 0.01$).

Mouse Subconjunctival Injection Study

Mouse experiments complied with the ARVO Statement for Use of Animals in Ophthalmic and Vision Research. Approval was obtained from the Institutional Animal Care and Use Committee (ARC-2019-020). Adult male mice (1–3 months) were housed and raised in air-filtered clear cages in a 12-hour light/dark cycle environment and fed as desired. Prox1-tdTomato mice (C57BL/6) are a reporter strain where lymphatic vessels can be conveniently visualized.[23]

Superior right eye 10 µL sub-conjunctival injections were performed using Hamilton syringes after intraperitoneal anesthesia (ketamine [100 mg/kg] and xylazine [5 mg/kg]) after which topical 0.3% ofloxacin ophthalmic solution was given. Two injections protocols were undertaken, "long" and "short." The long protocol took seven days with subconjunctival injections on days 1, 3, and 5. This was followed by euthanasia using carbon dioxide asphyxiation, cervical dislocation, and enucleation on day 7. The short protocol took three days with one subconjunctival injection on day 1. This was followed by carbon dioxide asphyxiation, cervical dislocation, and enucleation on day 3. Long protocol conditions included VEGFC (mouse recombinant vascular endothelial growth factor-C; BioLegend 775106; BioLegend, San Diego, CA, USA; n = 11 eyes; 0.36 mg/mL), pharmaceutical-grade mitomycin-C at two doses to asses dose-response (mitomycin-C; Accord Healthcare Inc, Durham, NC, USA; NDC 16729-115-05; n = 10 at 0.25 mg/mL and n = 9 at 0.5 mg/mL), pharmaceutical-grade 5FU (5-fluorouracil; Fresenius Kabi, Bad Homburg, Germany; NDC 63323-117-10; n = 10 at 50 mg/mL), and pharmaceutical-grade balanced salt solution (BSS; Alcon; NDC 0065-0795-50; n = 10) as a trauma control. For the short protocol, conditions included VEGFC (n = 8), MMC (n = 10 at each concentration), 5FU (n = 9), and BSS (n = 10). One short-protocol VEGFC injection mouse was excluded

Investigative Ophthalmology & Visual Science

because of conjunctival trauma during injection so that a bleb could not be formed. Non-injected controls (n = 10) were studied with the results compared to both protocols.

Enucleated eyes were fixed in 4% paraformaldehyde at 4°C for 2 to 4 hours and bisected with the lens and iris removed. The anterior halves were flattened using radial incisions, placed on a slide, and mounted with a cover slip. Fluorescent images were captured using a Zeiss ApoTome Microscope (Zeiss AxioVision software; Zeiss, Oberkochen, Germany). Subconjunctival lymphatic length (tracing the distance from the branch near Schlemm's canal to the distal end) and branch points (range 0–25) were quantified in a blinded fashion in each quadrant. Schlemm's canal was identified as a fluorescent, continuous, and circular structure around the limbus. Statistical comparisons were made by Mann-Whitney U test. To preserve an overall type-1 error rate of 0.05 and to statistically account for multiple comparisons, results were considered significant in mouse studies across the 15 comparisons if $P < 0.05/15 = 0.0033$ (Bonferroni correction; $P <$[acceptable P value]/[number of comparisons]). However, we also denoted results with a P value between 0.01 to 0.0033 to transparently demonstrate weaker effects that clearly overcame the standard 0.05 cutoff but that did not quite meet the stringent Bonferroni cut-off. All quantitative data are shown as mean ± SEM.

Results

Rabbit Experiments

To understand the morphology and distribution of rabbit subconjunctival bleb-related outflow pathways, one of two tracers was injected under the bulbar conjunctiva of rabbit eyes to form blebs (Figs. 1A–F, asterisks). Slit lamp and surgical microscope fluorescence photography showed that, after tracer injection, distinct bleb-related outflow pathways arose from the bleb edge (Figs. 1A–C [trypan blue] and D–F [fluorescent dextrans]). Multiple pathways could arise from each bleb, appear sausage-shaped, and display irregular branching (y-shaped, right-angle bends, or curvilinear routes) (Figs. 1A–F; black arrows). These pathways often coalesced to a smaller number of pathways or a single dominant route (Fig. 1; blue or yellow arrows). These subconjunctival outflow pathways did not co-localize with clearly visible ocular surface blood vessels.

To quantify subconjunctival bleb-related outflow pathways in rabbit eyes, trypan blue was injected on the temporal and nasal sides of 16 rabbit eyes (32 total blebs). Superior and inferior assessment was not performed because the eyelids blocked visualization. The number of pathways immediately extending from the blebs were counted (Figs. 1G–I). The average number of temporal and nasal

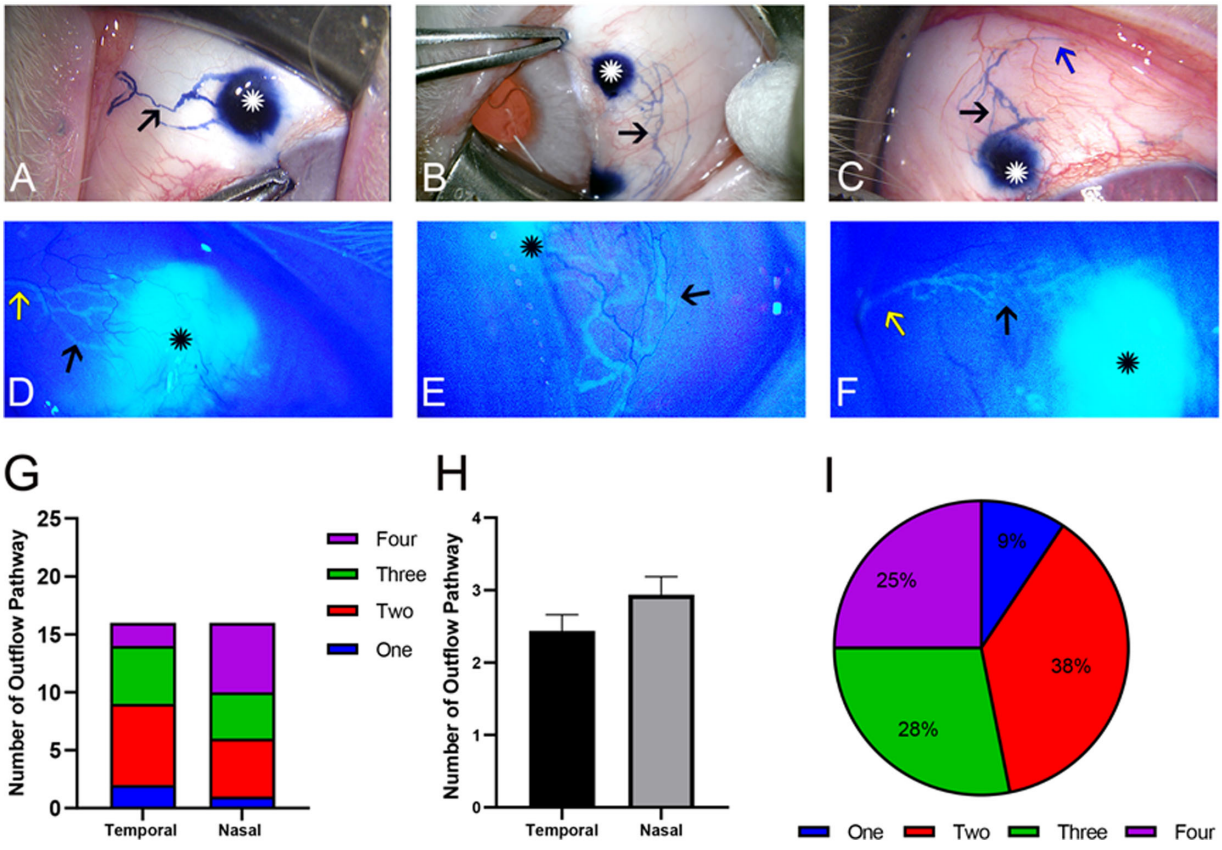

Figure 1. Qualitative appearance and quantitation of subconjunctival bleb-related outflow pathways in rabbit eyes. (**A–C**) Healthy rabbits receiving trypan blue blebs (*white asterisks*) showed initial bleb-related outflow pathways (*black arrows*), leading to a collecting vessel (*blue arrow*). (**D–F**) Healthy rabbits receiving FITC-dextran blebs (*black asterisks*) also showed initial bleb-related outflow pathways (*black arrows*) leading to collector vessels (*yellow arrows*). All images are of left eyes with (**E**) showing a nasal quadrant and the rest temporal. (**G**) The total number of outflow pathways arising from temporal or nasal blebs across all eyes were counted with the distribution of blebs showing 1, 2, 3, or 4 pathways denoted. (**H**) The average number of outflow pathways arising from temporal or nasal blebs. (**I**) Frequency of the number of pathways seen off all blebs (16 rabbit eyes, 32 total blebs).

Investigative Ophthalmology & Visual Science

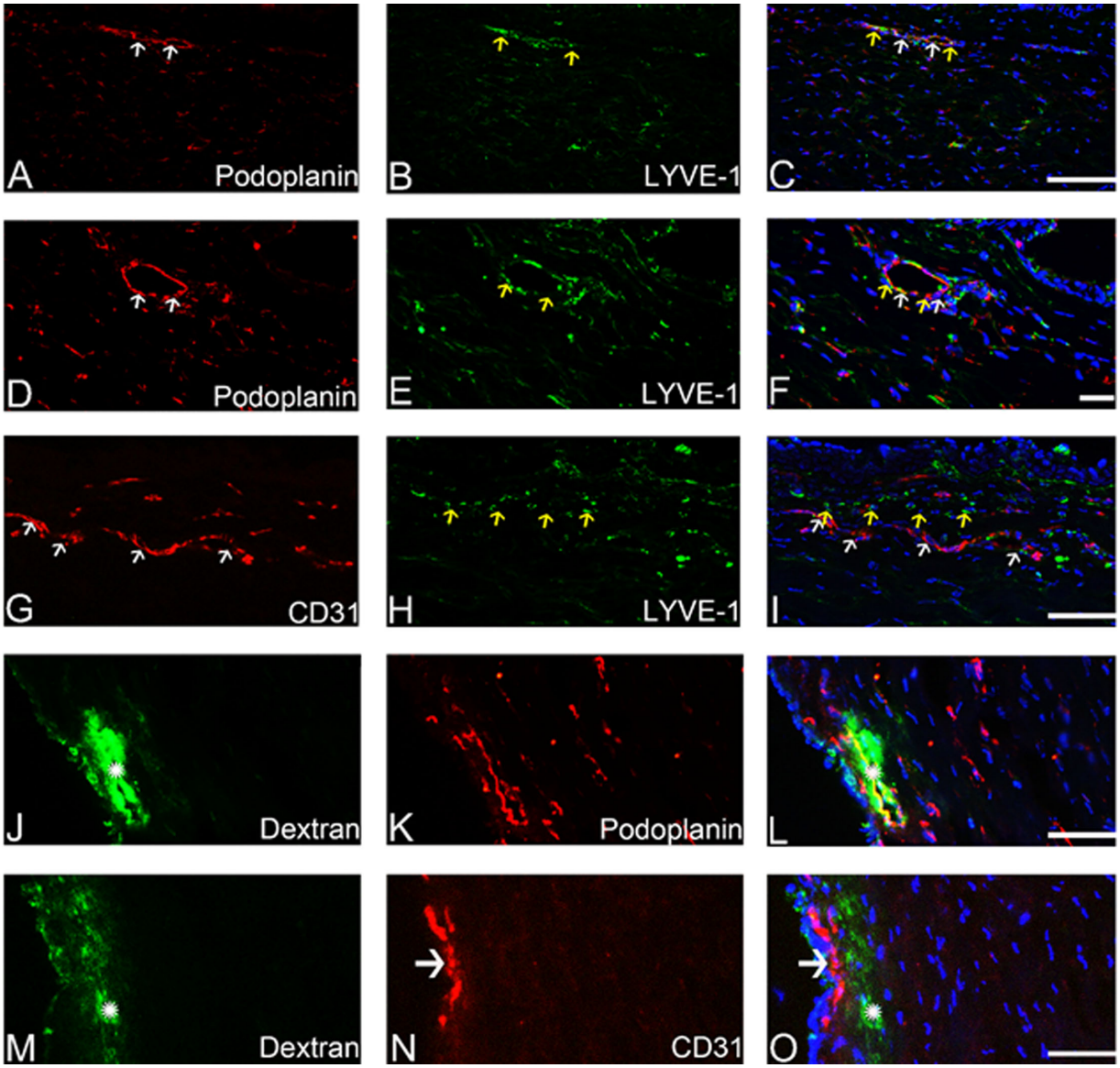

Figure 2. Immunofluorescence of lymphatic endothelial (Podoplanin and LYVE-1) and blood vessel (CD31) Makers. (**A–F**) Immunolabeling against lymphatic vessel markers podoplanin (*white arrows*) in (**A, D**) and LYVE-1 (*yellow arrows*) in (*B, E*) showed co-localization in (**C, F**) (*mixed white* and *yellow arrows*). (**G–I**) Immunolabeling against a lymphatic vessel marker LYVE-1 (*yellow arrows*) in (**H**) and a blood vessel endothelial marker CD31 (*white arrows*) in (**G**) did not show co-localization in (**I**) (*white* and *yellow arrows*). (**J, M**) After injection of fluorescent dextran blebs, outflow pathways were seen with trapped tracer lining outflow pathway lumens (*white asterisks*). (**K**) Immunolabeling on the same section against podoplanin, (**L**) showed co-localization with the tracer-labeled outflow pathway. (**N**) Immunolabeling on the same section against a blood vessel endothelial marker CD31, (**O**) did not show co-localization with the tracer-labeled outflow pathway. Instead, a distinct blood vessel (*white arrows*) was highlighted next to the bleb-related outflow pathway (*white asterisk*). *Scale bars*: 100 µm.

pathways were 2.44 ± 0.05 and 2.94 ± 0.06 (mean ± SEM), respectively. To determine if there was a temporal/nasal asymmetry (as per previous reports)[19,23] a paired t-test was performed with the null hypothesis that there was no overall difference between the nasal and temporal sides (Fig. 1H). The null hypothesis was not rejected ($P = 0.33$) suggesting that no asymmetry existed in rabbits. In all blebs, one pathway was seen in ~9% (3/32), two pathways in ~38% (12/32), three pathways in ~28% (9/32), and four pathways in ~25% (8/32) of blebs (Fig. 1I).

The dis-localization between bleb-related outflow pathways and blood vessels (Figs. 1A–F) suggested that these pathways were not blood vessels. To alternatively identify them, immunofluorescence was performed on isolated rabbit conjunctiva. In control tissues, immunofluorescence showed the presence of podoplanin positive pathways that co-localized with LYVE-1 (Figs. 2A–F), identifying putative lymphatics. LYVE-1 positive pathways further did not co-localize with CD31-positive blood vessels (Figs. 2G–I). Then, to uncover the identity of bleb-related outflow pathways, cases of FITC-dextran blebs were dissected and fixed. FITC-dextran bleb-related outflow pathways were thus re-identified on histological section (Figs. 2J, 2M). Replicating prior porcine results,[19] FITC-dextran pathways co-localized

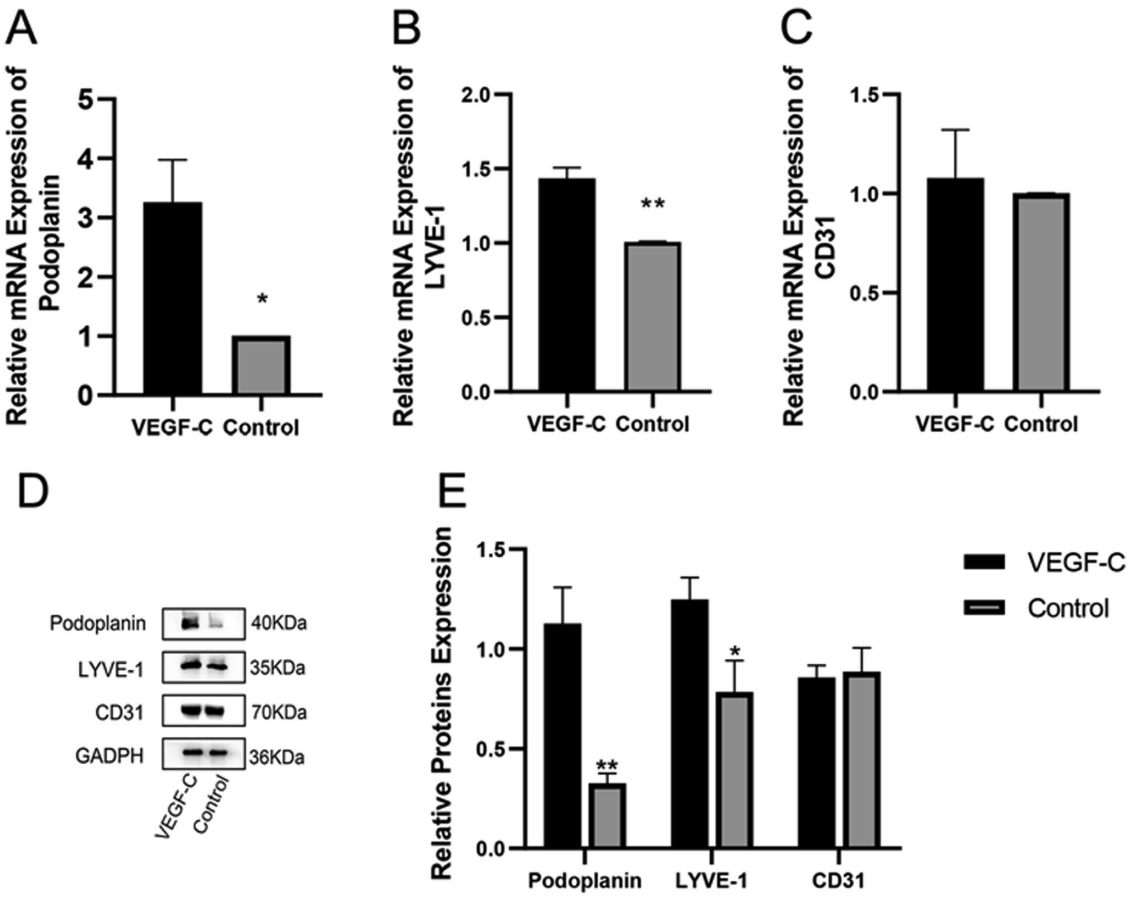

Figure 3. VEGFC Upregulates the Expression of Lymphatic Markers but not a Blood Vessel Endothelial Marker in Rabbit Conjunctiva. (**A–C**) After VEGFC subconjunctival injection, quantitative PCR from conjunctival lysate showed increased gene expression of lymphatic (LYVE-1 and podoplanin) markers but not a blood vessel (CD31) marker. (**D, E**) Western blot confirmed gene expression results with increased podoplanin and LYVE-1 protein but not CD31 after VEGFC injection relative to control (podoplanin, 40KDa; LYVE-1, 35KDa; CD31, 70KDa; and GADPH, 36KDa). *$P < 0.05$, **$P < 0.01$ versus control.

with podoplanin immunolabeling (Figs. 2J–L) but not CD31 immunolabeling (Figs. 2M–O).

We postulated that VEGFC can promote the proliferation of rabbit conjunctival lymphatics after subconjunctival injection. RT-qPCR quantitative analyses showed that mRNA expression levels of podoplanin (3.26 ± 0.61 relative expression) after VEGFC injection were significantly increased compared to control (1.00 ± 0.00) ($P = 0.03$) (Fig. 3A). mRNA expression levels of LYVE-1 (1.44 ± 0.07) was also significantly increased after VEGFC injection compared to control (1.01 ± 0.01) ($P = 0.004$) (Fig. 3B). However, there was no increase in CD31 blood vessel mRNA levels between VEGFC (1.07 ± 0.21) and control (1.00 ± 0.00) ($P = 0.77$) (Fig. 3C). These results were confirmed using Western blot semi-quantitative analyses which showed increased protein levels of podoplanin (1.16 ± 0.19) in conjunctiva injected with VEGFC compared to control (0.3 ± 0.03) ($P = 0.01$) (Figs. 3D, 3E). Expression level of LYVE-1 protein (1.28 ± 0.08) was also significantly increased after VEGFC injection compared to control (0.77 ± 0.15) ($P = 0.04$) (Figs. 3D, 3E). However, the expression level of CD31 protein was not significantly different between the VEGFC (0.86 ± 0.06) and control (0.89 ± 0.12) ($P = 0.84$) (Figs. 3D, 3E).

Mouse Experiments

A mouse model was then used for subsequent study because of the ability to more easily generate many animals and because a mouse reporter strain with natively fluorescent subconjunctival lymphatics was available. With the ability to generate more mice, two separate injection protocols ("short" and "long") were tested in addition to assessing putative pro-lymphatic factors (VEGFC) and possible anti-lymphatic factors (5FU and MMC at two doses). Qualitatively, subconjunctival lymphatics were visible (Fig. 4). After the "short protocol", subconjunctival lymphatics were seen, but no obvious qualitative difference was seen across conditions (Figs. 4A–F). After the "long protocol," injection of BSS alone as a trauma control had a mild positive qualitative impact (Fig. 4H) on lymphangiogenesis compared to a non-injection control. VEGFC-induced lymphangiogenesis was more profound (Fig. 4I). Anti-metabolites appeared to qualitatively diminish lymphatic presence, particularly at the higher MMC dose (Figs. 4J–L).

Quantitatively, the number of subconjunctival branch points and branch lengths were measured. The "long" protocol demonstrated statistically significant changes (Figs. 5A–H). Overall, the results demonstrated that BSS injection induced partial lymphangiogenesis compared to the "no

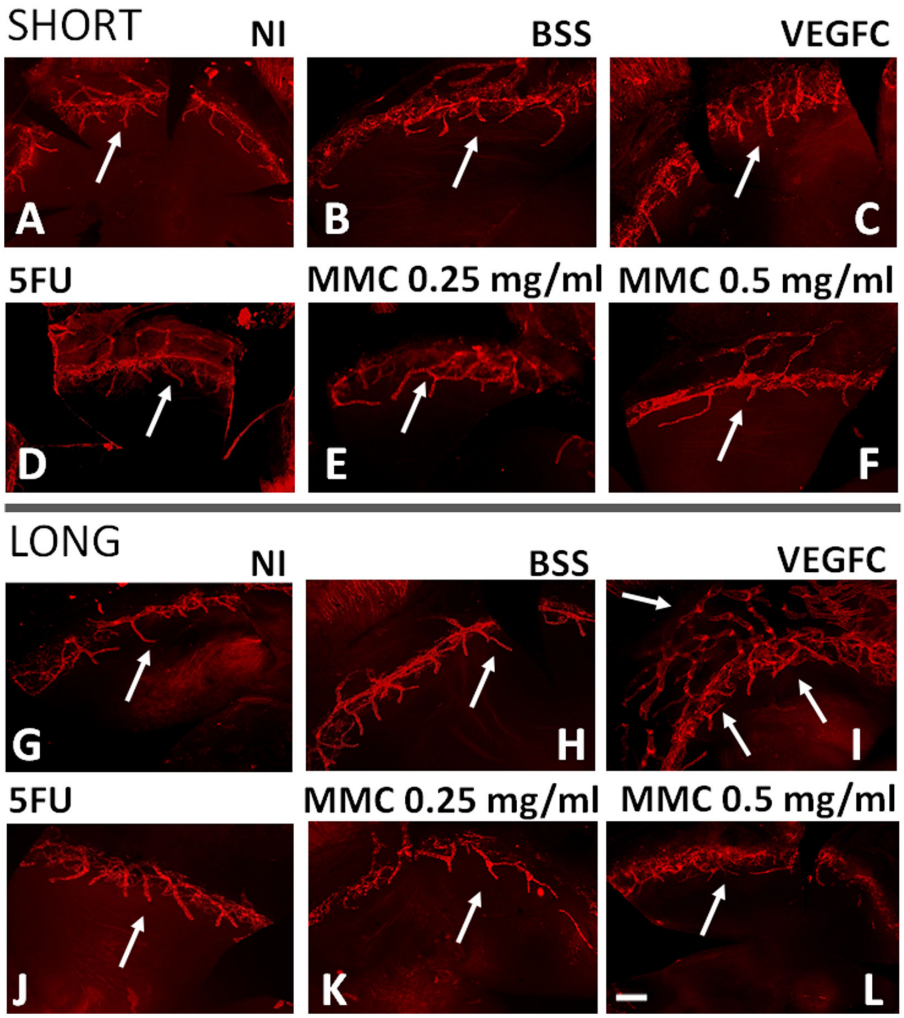

Figure 4. Mouse Subconjunctival Lymphatic Manipulation. (**A–F**) Short Protocol: injection on day 1 with tissue acquisition on day 3. (**G–L**) Long Protocol: injection on days 1, 3, and 5 with tissue acquisition on day 7. Subconjunctival lymphatics (*white arrows*). NI, no injection. *Scale bar*: 100 µm.

injection" condition as an indication of trauma-induced lymphangiogenesis (superior branch data: no injection [8.7 ± 0.8] vs. BSS [12.1 ± 0.8], $P = 0.007$) (superior length data: no injection [224.9 ± 13.9 microns] vs. BSS [271.7 ± 15.6 µm]; $P = 0.062$). VEGFC induced greater lymphangiogenesis (superior branch data: VEGFC [18 ± 1.5] vs. BSS [12.1 ± 0.8], $P = 0.004$) (superior length data: VEGFC [357.1 ± 13.8 µm] vs. BSS [271.7 ± 15.6 µm]; $P < 0.001$). Anti-metabolite diminished lymphangiogenesis in some cases with a potential trend for greater effect at the higher MMC dose (Figs. 5A–H). There was also a locational effect. All injections were superior, and a greater number of statistically significant changes (black or orange bars) were seen in that quadrant (Figs. 5A–E). However, superior subconjunctival injections can spread to other quadrants of the eye for off-locational effects that were still present but less consistent (fewer black or orange bars) (Figs. 5B–D and 5F–H) in other areas. The "short protocol" was performed to provide further information about the impact of time and number of injections. In this case, there were no statistically significant changes amongst any comparisons for branch number (Figs. 6A–D) or length (Figs. 6E–H) at either a $P < 0.0033$ (Bonferroni-corrected) or $P = 0.01$–0.003 level.

Given the number and complexity of comparisons, we sought to transparently show all P values, color-coded to provide a complete picture (Figs. 7A, 7B). We included standard significance cut-offs ($P < 0.05$) in addition to the Bonferroni cut-off for all comparisons with green and red denoting statistical significance or lack thereof, respectively. Clusters of green highlighted results with greater confidence. Overall, the top horizontal green bands (Figs. 7A, 7B) depicted a consistent positive impact of VEGFC on lymphangiogenesis. The green clusters on the left of the tables (Figs. 7A, 7B, yellow box) demonstrated a lesser impact of anti-metabolites on lymphatic suppression.

Discussion

Rabbit and mouse subconjunctival lymphatics were characterized. Moreover, we showed the ability to pharmacologically influence subconjunctival lymphatics in both a positive and negative direction in these two mammalian species. Bleb-related outflow pathways appeared in the rabbit. These pathways were clearly not blood vessels because they did not co-localize with either visible blood vessels or blood vessel-specific CD-31 immunolabeled

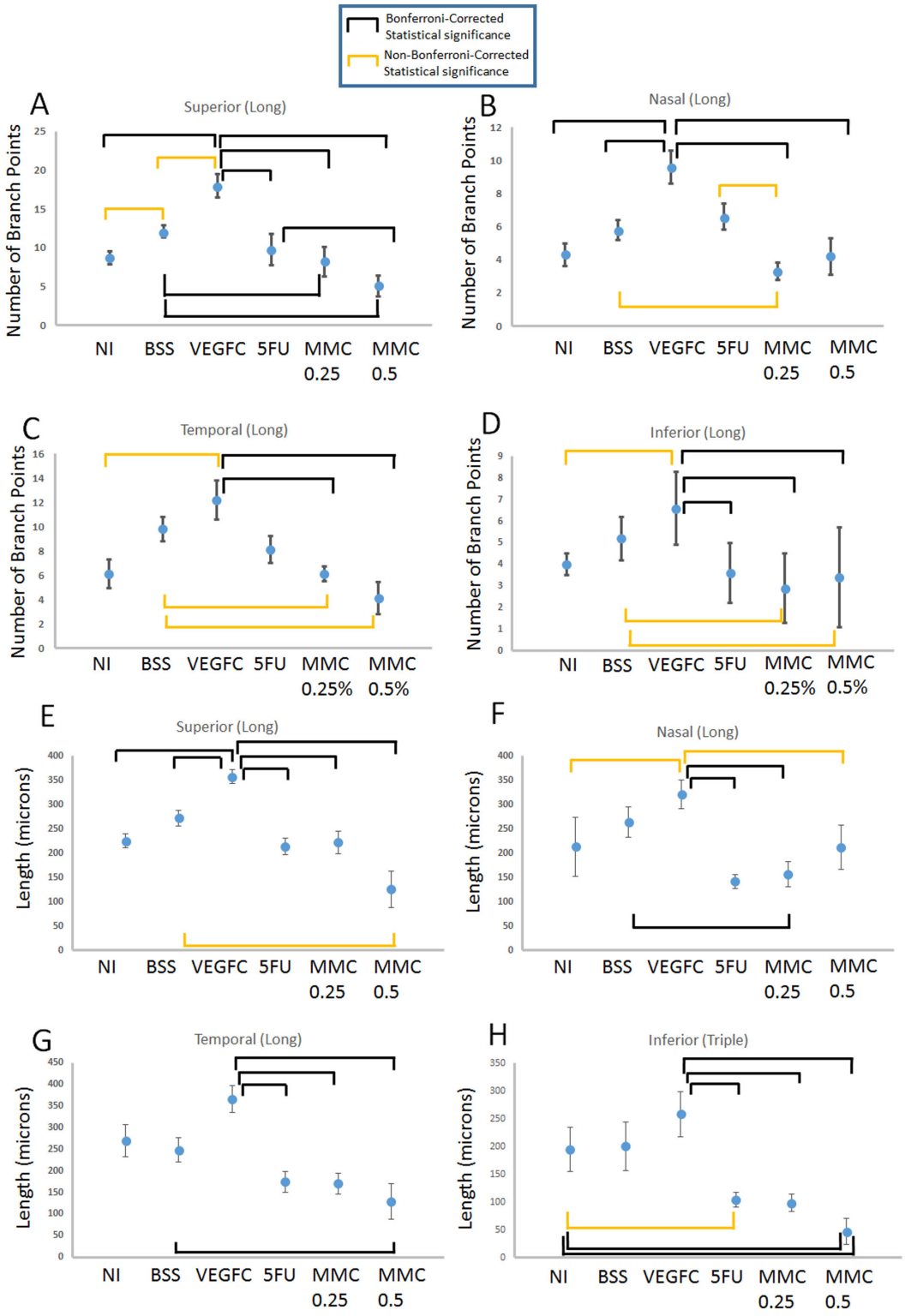

Figure 5. Subconjunctival branch and length measurements with long injection protocol. Black comparisons ($P < 0.0033$; Bonferroni-corrected). Orange comparisons ($P = 0.01$–0.003). Superior, nasal, temporal, and Inferior are different quadrants of the eye. NI, no injection. MMC units are mg/mL.

pathways. Then, a lymphatic identity was confirmed for rabbit bleb-related outflow pathways with lymphatic endothelial markers (podoplanin and LYVE-1) using similar methods previously described for porcine eyes.[19] Subconjunctival injection of VEGFC then increased the rabbit lymphatic presence as assessed by podoplanin and LYVE-1 mRNA and protein levels with no impact on CD31. Our investigation also confirmed these results in the mouse

Investigative Ophthalmology & Visual Science

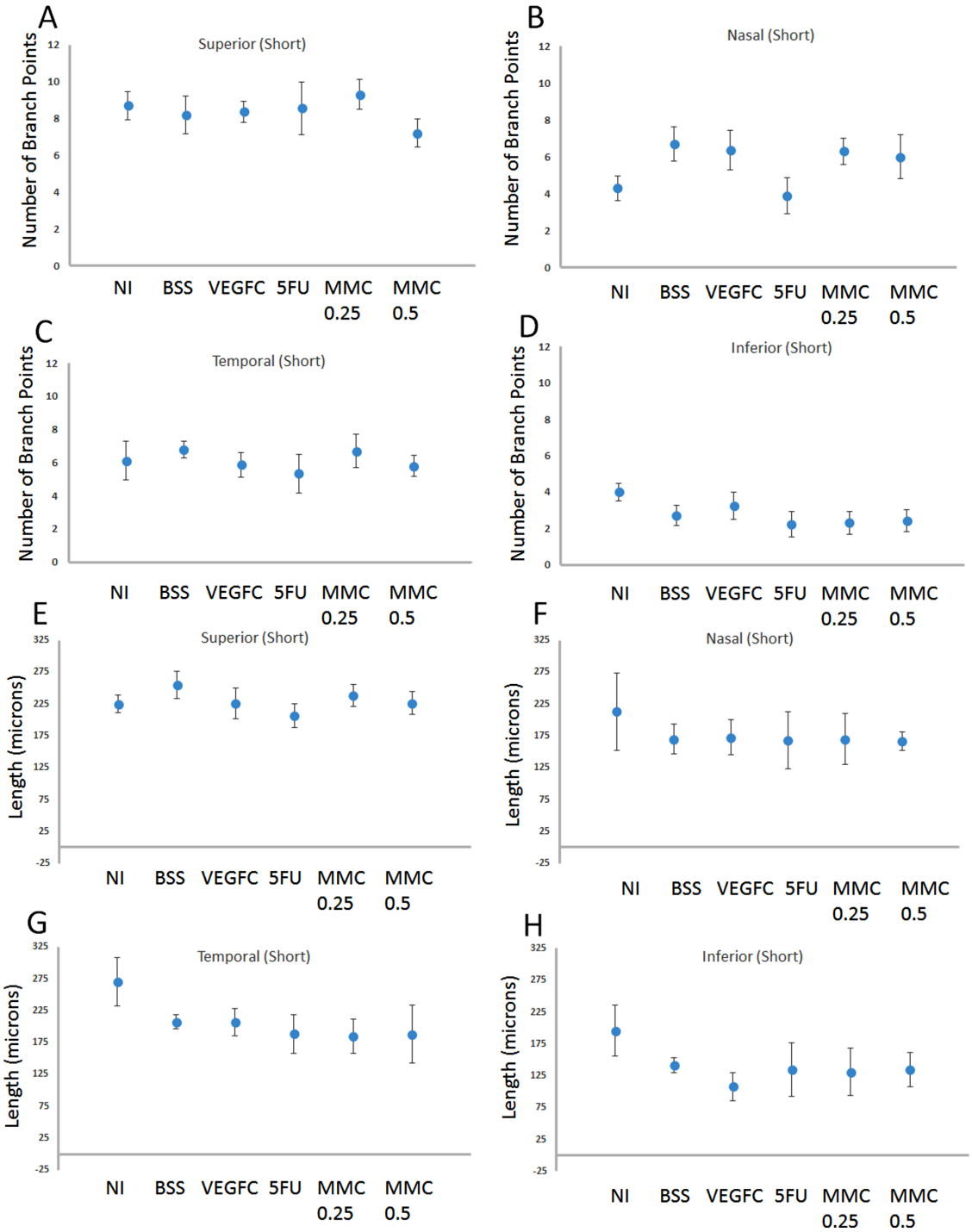

Figure 6. Subconjunctival branch and length measurements with short injection protocol. Superior, nasal, temporal, and inferior are different quadrants of the eye. NI, no injection. MMC units are mg/ml.

using a different approach. In the subconjunctival lymphatic reporter mouse, VEGFC and anti-metabolite increased and decreased lymphatic presence, respectively.

Acquiring consistent data between two species adds strength to the conclusions and acknowledges that species-specific differences exist. Rabbit is a good model to study subconjunctival outflow because trabeculectomy studies are performed in rabbits with primary endpoints including surgical bleb survival or physical bleb characteristics.[21,22] However, it can be difficult to study rabbits given cost, time, and a lack of suitable reagents. For example, fewer antibodies are validated against rabbit antigens. Moreover, some primary antibodies are created in rabbits leading to difficult immunolabeling. In contrast, mice are advantageous as many more animals can be generated in a shorter amount of time. The presence of genetic models, such as the subconjunctival lymphatic reporter mouse used in this report,[23] allowed the same questions as assessed in rabbits to be queried using

Investigative Ophthalmology & Visual Science

A

Branch Data

	Superior p<0.05	Nasal p<0.05	Temporal p<0.05	Inferior p<0.05	Superior BC	Nasal BC	Temporal BC	Inferior BC
VEGFC vs. No Injection	<0.001	<0.001	0.005	0.004	<0.001	<0.001	0.005	0.004
VEGFC vs. BSS	0.004	0.003	0.314	0.061	0.004	0.003	0.314	0.061
VEGFC vs. 5FU	<0.001	0.043	0.043	0.001	<0.001	0.043	0.043	0.001
VEGFC vs. MMC 0.25%	<0.001	<0.001	<0.001	<0.001	<0.001	<0.001	<0.001	<0.001
VEGFC vs. MMC 0.5%	<0.001	0.003	0.001	0.003	<0.001	0.003	0.001	0.003
No injection vs. BSS	0.007	0.165	0.043	0.089	0.007	0.165	0.043	0.089
No injection vs 5FU	0.218	0.052	0.28	0.631	0.218	0.052	0.28	0.631
No injection vs. MMC 0.25%	0.631	0.28	0.853	0.123	0.631	0.28	0.853	0.123
No injection vs. MMC 0.5%	0.065	0.842	0.243	0.278	0.065	0.842	0.243	0.278
BSS vs. 5FU	0.015	0.436	0.436	0.015	0.015	0.436	0.436	0.015
BSS vs. MMC 0.25%	0.002	0.007	0.009	0.004	0.002	0.007	0.009	0.004
BSS vs. MMC 0.5%	<0.001	0.278	0.004	0.008	<0.001	0.278	0.004	0.008
5FU vs. MMC 0.25%	0.075	0.005	0.089	0.28	0.075	0.005	0.089	0.28
5FU vs. MMC 0.5%	0.003	0.133	0.035	0.4	0.003	0.133	0.035	0.4
MMC 0.25% vs. MMC 0.5%	0.156	0.604	0.182	0.604	0.156	0.604	0.182	0.604

B

Length Data

	Superior p<0.05	Nasal p<0.05	Temporal p<0.05	Inferior p<0.05	Superior BC	Nasal BC	Temporal BC	Inferior BC
VEGFC vs. No Injection	<0.001	0.005	0.024	0.085	<0.001	0.005	0.024	0.085
VEGFC vs. BSS	<0.001	0.152	0.02	0.114	<0.001	0.152	0.02	0.114
VEGFC vs. 5FU	<0.001	<0.001	<0.001	0.001	<0.001	<0.001	<0.001	0.001
VEGFC vs. MMC 0.25%	<0.001	<0.001	<0.001	0.001	<0.001	<0.001	<0.001	0.001
VEGFC vs. MMC 0.5%	<0.001	0.006	0.001	<0.001	<0.001	0.006	0.001	<0.001
No injection vs. BSS	0.063	0.075	0.631	0.971	0.063	0.075	0.631	0.971
No injection vs 5FU	0.393	0.971	0.023	0.009	0.393	0.971	0.023	0.009
No injection vs. MMC 0.25%	0.631	0.353	0.023	0.015	0.631	0.353	0.023	0.015
No injection vs. MMC 0.5%	0.053	0.604	0.013	0.003	0.053	0.604	0.013	0.003
BSS vs. 5FU	0.015	0.019	0.105	0.019	0.015	0.019	0.105	0.019
BSS vs. MMC 0.25%	0.075	0.003	0.089	0.035	0.075	0.003	0.089	0.035
BSS vs. MMC 0.5%	0.004	0.043	0.002	0.001	0.004	0.043	0.002	0.001
5FU vs. MMC 0.25%	0.912	0.529	0.971	0.436	0.912	0.529	0.971	0.436
5FU vs. MMC 0.5%	0.095	0.968	0.079	0.156	0.095	0.968	0.079	0.156
MMC 0.25% vs. MMC 0.5%	0.079	0.905	0.243	0.243	0.079	0.905	0.243	0.243

Figure 7. Statistical significance across all conditions in long protocol. superior, nasal, temporal, and inferior are different quadrants of the eye. NI, no injection; BC, Bonferroni correction. P value < 0.0033. Green and red cells are significant and non-significant by $P < 0.05$ or BC cutoffs, respectively.

a completely different approach. Overall, results in both species clearly demonstrated that VEGFC increased subconjunctival lymphatic mRNA, proteins, and/or presence. At the same time, differences between the species were noted. For example, rabbits in this study did not show a subconjunctival lymphatic predilection for the nasal side of the eye that has been reported in pig[19] and mouse[23] eyes. Thus our research supports the potential of lymphatic manipulation in two species while also demonstrating that species-specific differences can exist.

Statistical transparency is a strength of this study. Mouse work used a greater number of animals that were simultaneously compared. Bonferroni statistical correction is a strategy to mitigate the acceptance of significant P values arising due to random chance. Although commonly used in clinical sciences, it is sometimes avoided in laboratory studies which instead use the standard significance cutoff of $P < 0.05$. The significance cutoff for a Bonferroni corrected P value can be a daunting hurdle, $P < 0.0033$ for the multiple comparison experiments in this article (Figs. 5–7). We previously reported on subconjunctival lymphatics[19] using this strict benchmark and continue to do so here. However, a high hurdle to avoid false-positive statistical significance also simultaneously risks false negative conclusions (missing a true, but smaller magnitude finding). Therefore, we further described our results with a $P = 0.01$–0.0033 cutoff (Figs. 5, 6). Although not meeting Bonferroni standards, we point out that results within this P value range showed biological plausibility. For instance, comparisons in this range between VEGFC to NI or BSS were positioned with VEGFC showing greater lymphatic length or branch number as opposed to less. This lends additional credibility to those P values (such as $P = 0.001$). Additional biological plausibility for the results occurred in the observed trend of greater frequency and magnitude of statistical significance in the superior quadrant compared to the other quadrants. This makes sense because, although drugs can diffuse to other locations, the injections were all superior. We lastly showed all P values for all comparisons (both standard $P < 0.05$ and Bonferroni cutoffs) to transparently display the trends and common conclusions among the results (Fig. 7).

Investigative Ophthalmology & Visual Science

One such conclusion was that VEGFC potently promotes lymphangiogenesis. On the surface, this should not be surprising as VEGFC belongs to a group of proteins that proliferate blood and lymphatic vessels. VEGFs type A and B are well known to promote blood vessel growth, be involved in ocular neovascularization, and represent the targets of anti-VEGF therapy used in conditions such as age-related macular degeneration[36] and neovascular glaucoma.[26] VEGF type-C,[26,37] however, promotes lymphatic growth, and certain mutations (VEGFC-C156S)[38] are particularly specific for lymphatics. VEGFC has been shown to promote lymphangiogenesis in other experimental systems and areas of the body such as chick chorioallantoic membrane[37] and mammalian gut mesentery.[39] Therefore molecular pathways exist to modify lymphatics. We speculate that VEFGC-induced lymphangiogenesis may be a strategy to improve bleb outflow for bleb-requiring glaucoma surgeries. All glaucoma surgeons have seen cases where surgical blebs persist after bleb-requiring glaucoma surgeries (suggesting that the pathway between the anterior chamber and subconjunctival space is not impeded by a fibroproliferative scar) but that the eye pressure is still high (suggesting that aqueous is trapped in a bleb cul-du-sac and unable to escape). Current clinical data suggest that lymphatic-like pathways may be associated with better glaucoma surgical outcomes.[28,40] Thus future studies will be performed to test the impact of VEGFC on trabeculectomy models.

Another conclusion from this work is that antimetabolites diminish the presence of lymphatics, as previously hypothesized.[27] Trabeculectomies are almost always performed with antimetabolites.[41,42] Failed trabeculectomy blebs after antimetabolite exposure have been shown to be without lymphatics whereas conjunctiva next to failed blebs have an intermediate lymphatic presence.[43] Antimetabolites block DNA synthesis. The act of trauma (e.g., from surgeries or injections) is itself a driver of lymphangiogenesis. Thus blocking DNA synthesis in a setting of lymphatic growth that requires DNA turnover may be the mechanism by how antimetabolites lead to diminished or altered lymphatics. Further research needs to be performed to test the impact of limiting subconjunctival lymphatics. Doing so may be one strategy to improve the efficacy of subconjunctival drug delivery by limiting drug egress from that space after drug injection.

In conclusion, the current study characterized rabbit and mouse lymphatics in ocular surface tissue. It demonstrates that subconjunctival lymphatic presence can be influenced in positive and negative ways using different experimental approaches from two mammalian species. The primary emphasis was to test for changes to subconjunctival lymphatics at a molecular (mRNA or protein) and structural level in a larger number of conditions to increase the validity of the results. Future studies are needed to study the impact of subconjunctival lymphatic alteration on functional endpoints such as in glaucoma surgical bleb models or subconjunctival drug delivery studies.

Acknowledgments

Supported by the National Institutes of Health, Bethesda, MD (Grant Numbers R01EY030501 [ASH], R21EY026260 [YH], R01EY029058 [RNW]; Glaucoma Research Foundation Shaffer Grant [AH]; an unrestricted grant from Research to Prevent Blindness (New York, NY) [UCSD]; Natural Science Foundation of Shandong Province (No. ZR2020MH172); the Demonstration and Guidance Project of Science and Technology Benefiting People in Qingdao (No.20-3-4-39-nsh).

Disclosure: **J.Y. Lee,** None; **J. Wu,** None; **Y. Liu,** None; **S. Saraswathy,** None; **L. Zhou,** None; **Q. Bu,** None; **Y. Su,** None; **D. Choi,** None; **E. Park,** None; **C.A. Strohmaier,** None; **R.N. Weinreb,** None; **Y.-K. Hong,** None; **X. Pan,** None; **A.S. Huang,** Allergan/Abbvie (C), Celanese (C), Diagnosys: Research Support Equinox (C), Glaukos Corporation: Research Support (C), Gore (C), Heidelberg Engineering: Research Support Qlaris (C), Santen Pharmaceuticals (C), Topcon (C)

References

1. Grixti A, Sadri M, Edgar J, Datta AV. Common ocular surface disorders in patients in intensive care units. *Ocul Surf*. 2012;10:26–42.
2. Azari AA, Arabi A. Conjunctivitis: A Systematic Review. *J Ophthalmic Vis Res*. 2020;15:372–395.
3. Sanders R, MacEwen CJ, Haining WM. A comparison of prophylactic, topical and subconjunctival treatment in cataract surgery. *Eye (Lond)*. 1992;6(Pt 1):105–110.
4. Sohn EH, Wang R, Read R, et al. Long-term, multicenter evaluation of subconjunctival injection of triamcinolone for non-necrotizing, noninfectious anterior scleritis. *Ophthalmology*. 2011;118:1932–1937.
5. Cairns JE. Trabeculectomy. Preliminary report of a new method. *Am J Ophthalmol*. 1968;66:673–679.
6. Gedde SJ, Singh K, Schiffman JC, Feuer WJ, Group TVTS. The Tube Versus Trabeculectomy Study: interpretation of results and application to clinical practice. *Curr Opin Ophthalmol*. 2012;23:118–126.
7. Oliver G, Kipnis J, Randolph GJ, Harvey NL. The lymphatic vasculature in the 21. *Cell*. 2020;182:270–296.
8. Yucel YH, Johnston MG, Ly T, et al. Identification of lymphatics in the ciliary body of the human eye: A novel "uveolymphatic" outflow pathway. *Exp Eye Res*. 2009;89:810–819.
9. Aspelund A, Antila S, Proulx ST, et al. A dural lymphatic vascular system that drains brain interstitial fluid and macromolecules. *J Exp Med*. 2015;212:991–999.
10. Kaser-Eichberger A, Schrödl F, Trost A, et al. Topography of lymphatic markers in human iris and ciliary body. *Invest Ophthalmol Vis Sci*. 2015;56:4943–4953.
11. Narayanaswamy A, Thakur S, Nongpiur ME, et al. Aqueous outflow channels and its lymphatic association: A review. *Surv Ophthalmol*. 2021;67:659–674.
12. Yu DY, Morgan WH, Sun X, et al. The critical role of the conjunctiva in glaucoma filtration surgery. *Prog Retin Eye Res*. 2009;28:303–328.
13. Guo W, Zhu Y, Yu PK, et al. Quantitative study of the topographic distribution of conjunctival lymphatic vessels in the monkey. *Exp Eye Res*. 2012;94:90–97.
14. Schroedl F, Kaser-Eichberger A, Schlereth SL, et al. Consensus statement on the immunohistochemical detection of ocular lymphatic vessels. *Invest Ophthalmol Vis Sci*. 2014;55:6440–6442.
15. Grüntzig J, Hollmann F. Lymphatic vessels of the eye—old questions—new insights. *Ann Anat*. 2019;221:1–16.
16. Freitas-Neto CA, Costa RA, Kombo N, et al. Subconjunctival indocyanine green identifies lymphatic vessels. *JAMA Ophthalmol*. 2015;133:102–104.
17. Lee JY, Heilweil G, Le P, et al. Structural confirmation of lymphatic outflow from subconjunctival blebs of live human subjects. *Ophthalmol Sci*. 2021;1(4):100080.
18. Huang AS, Belghith A, Dastiridou A, Chopra V, Zangwill LM, Weinreb RN. Automated circumferential construction of first-order aqueous humor outflow pathways using

spectral-domain optical coherence tomography. *J Biomed Opt*. 2017;22:66010.

19. Akiyama G, Saraswathy S, Bogarin T, et al. Functional, structural, and molecular identification of lymphatic outflow from subconjunctival blebs. *Exp Eye Res*. 2020;196:108049.
20. Gong P, Yu DY, Wang Q, et al. Label-free volumetric imaging of conjunctival collecting lymphatics ex vivo by optical coherence tomography lymphangiography. *J Biophotonics*. 2018;11:e201800070.
21. Memarzadeh F, Varma R, Lin LT, et al. Postoperative use of bevacizumab as an antifibrotic agent in glaucoma filtration surgery in the rabbit. *Invest Ophthalmol Vis Sci*. 2009;50:3233–3237.
22. Ozgonul C, Mumcuoglu T, Gunal A. The effect of bevacizumab on wound healing modulation in an experimental trabeculectomy model. *Curr Eye Res*. 2014;39:451–459.
23. Wu Y, Seong YJ, Li K, et al. Organogenesis and distribution of the ocular lymphatic vessels in the anterior eye. *JCI Insight*. 2020;5(13):e135121.
24. Norden PR, Sabine A, Wang Y, et al. Shear stimulation of FOXC1 and FOXC2 differentially regulates cytoskeletal activity during lymphatic valve maturation. *Elife*. 2020;9:e53814.
25. Leppänen VM, Tvorogov D, Kisko K, et al. Structural and mechanistic insights into VEGF receptor 3 ligand binding and activation. *Proc Natl Acad Sci USA*. 2013;110:12960–12965.
26. Rauniyar K, Jha SK, Jeltsch M. Biology of Vascular Endothelial Growth Factor C in the Morphogenesis of Lymphatic Vessels. *Front Bioeng Biotechnol*. 2018;6:7.
27. Singh D. Conjunctival lymphatic system. *J Cataract Refract Surg*. 2003;29:632–633.
28. Khoo YJ, Abdullah AAH, Yu DY, Morgan WH. Use of trypan blue to assess lymphatic function following trabeculectomy. *Clin Exp Ophthalmol*. 2019;47:892–897.
29. Saraswathy S, Tan JC, Yu F, et al. Aqueous Angiography: real-time and physiologic aqueous humor outflow imaging. *PLoS One*. 2016;11:e0147176.
30. Huang AS, Saraswathy S, Dastiridou A, et al. Aqueous angiography-mediated guidance of trabecular bypass improves angiographic outflow in human enucleated eyes. *Invest Ophthalmol Vis Sci*. 2016;57:4558–4565.
31. Huang AS, Saraswathy S, Dastiridou A, et al. Aqueous angiography with fluorescein and indocyanine green in bovine eyes. *Transl Vis Sci Technol*. 2016;5:5.
32. Breiteneder-Geleff S, Matsui K, Podoplanin A S., novel 43-kd membrane protein of glomerular epithelial cells, is down-regulated in puromycin nephrosis. *Am J Pathol*. 1997;151:1141–1152.
33. Cursiefen C, Schlötzer-Schrehardt U, Küchle M. Lymphatic vessels in vascularized human corneas: Immunohistochemical investigation using LYVE-1 and podoplanin. *Invest Ophthalmol Vis Sci*. 2002;43:2127–2135.
34. Nakao S, Zandi S, Faez S, Kohno R, Hafezi-Moghadam A. Discontinuous LYVE-1 expression in corneal limbal lymphatics: dual function as microvalves and immunological hot spots. *The FASEB Journal*. 2011;26:808–817.
35. Chen L, Cursiefen C, Barabino S, Zhang Q, Dana MR. Novel expression and characterization of lymphatic vessel endothelial hyaluronate receptor 1 (LYVE-1) by conjunctival cells. *Invest Ophthalmol Vis Sci*. 2005;46:4536–4540.
36. Martin DF, Maguire MG, Ying GS, et al. Ranibizumab and bevacizumab for neovascular age-related macular degeneration. *N Engl J Med*. 2011;364:1897–1908.
37. Oh SJ, Jeltsch MM, Birkenhäger R, et al. VEGF and VEGF-C: specific induction of angiogenesis and lymphangiogenesis in the differentiated avian chorioallantoic membrane. *Dev Biol*. 1997;188:96–109.
38. Joukov V, Kumar V, Sorsa T, et al. A recombinant mutant vascular endothelial growth factor-C that has lost vascular endothelial growth factor receptor-2 binding, activation, and vascular permeability activities. *J Biol Chem*. 1998;273:6599–6602.
39. Sweat RS, Sloas DC, Murfee WL. VEGF-C induces lymphangiogenesis and angiogenesis in the rat mesentery culture model. *Microcirculation*. 2014;21:532–540.
40. Lenzhofer M, Strohmaier C, Hohensinn M, et al. Longitudinal bleb morphology in anterior segment OCT after minimally invasive transscleral ab interno Glaucoma Gel Microstent implantation. *Acta Ophthalmol*. 2018;97(2):e231–e237.
41. Palanca-Capistrano AM, Hall J, Cantor LB, Morgan L, Hoop J, WuDunn D. Long-term outcomes of intraoperative 5-fluorouracil versus intraoperative mitomycin C in primary trabeculectomy surgery. *Ophthalmology*. 2009;116:185–190.
42. Wong TT, Khaw PT, Aung T, et al. The Singapore 5-Fluorouracil Trabeculectomy Study: Effects on intraocular pressure control and disease progression at 3 years. *Ophthalmology*. 2009;116:175–184.
43. Bouhenni RA, Al Jadaan I, Rassavong H, et al. Lymphatic and blood vessel density in human conjunctiva after glaucoma filtration surgery. *J Glaucoma*. 2016;25:e35–e38.

Investigative Ophthalmology & Visual Science